Magnetic behaviors of cerium oxide-based thin films deposited using electrochemical method*

Peng Ying-Zi(彭英姿)[a)b)†], Li Yuan(李 源)[a)b)], Bai Ru(白 茹)[b)], Huo De-Xuan(霍德璇)[b)c)], and Qian Zheng-Hong(钱正洪)[b)]

[a)] School of Science, Hangzhou Dianzi University, Hangzhou 310018, China
[b)] Center for Integrated Spintronic Devices, Hangzhou Dianzi University, Hangzhou 310018, China
[c)] College of Materials and Environmental Engineering, Hangzhou Dianzi University, Hangzhou 310018, China

(Received 5 January 2014; revised manuscript received 3 April 2014; published online 23 July 2014)

Zn and Co multi-doped CeO_2 thin films have been prepared using an anodic electrochemical method. The structures and magnetic behaviors are characterized by several techniques, in which the oxygen states in the lattice and the absorptive oxygen bonds at the surface are carefully examined. The absorptive oxygen bond is about 50% of the total oxygen bond by using a semi-quantitative method. The value of actual stoichiometry δ' is close to 2. The experimental results indicate that the thin films are of a cerium oxide-based solid solution with few oxygen vacancies in the lattice and many absorptive oxygen bonds at the surface. Week ferromagnetic behaviors were evidenced by observed M–H hysteresis loops at room temperature. Furthermore, an evidence of relative ferromagnetic contributions was revealed by the temperature dependence of magnetization. It is believed that the ferromagnetic contributions exhibited in the M–H loops originate from the absorptive oxygen on the surface rather than the oxygen vacancies in the lattice.

Keywords: cerium oxide-based thin films, anodic electrochemical method, absorptive oxygen, magnetic behaviors

PACS: 75.50.Pp, 82.45.Aa, 68.55.–a, 75.70.–i **DOI:** 10.1088/1674-1056/23/9/097503

1. Introduction

In the last few years, since the discovery of room-temperature ferromagnetism (RTFM) in transparent transition metal-doped titanium dioxide, the diluted magnetic oxides (DMOs)-based materials have attracted much scientific attention. As both charge and spin degrees of freedom can be manipulated in DMOs-based materials, it is believed that such materials have potential applications in the spintronics and magneto–optics fields. Concerning the RTFM, many experimental results have been reported, such as ZnO, TiO_2, SnO_2, In_2O_3, and CeO_2-based materials, particularly of the doping effect when they were doped with 3d transition metal (TM) ions.[1] As one of such promising candidates, ceria crystals doped with TM ions are of interest.[2–8] RTFM in single crystal $Ce_{1-x}Co_xO_2$ ($x \leq 0.05$) films deposited on a $LaAlO_3$ (001) substrate by a pulsed laser deposition technique,[4] as first reported by Tiwari *et al.*, the films exhibited a very high Curie temperature about 740–875 K with a giant magnetic moment; the ferromagnetic property is intrinsic for the CeO_2 system, rather than a result of any secondary magnetic phase or cluster formation. Later, there are other experiments conducted with similar results. For example, $Ce_{1-x}Fe_xO_{2-\delta}$/LaAlO3 (001) thin films ($x = 0.01$ and 0.03) have been prepared by the pulsed laser deposition method.[5] RTFM is confirmed by the isothermal hysteresis as well as temperature-dependent magnetization measurements, which clearly show it has a ferromagnetic Curie temperature of at least more than 350 K. Meanwhile paramagnetic and superferromagnetic behaviors were also reported.[9,10] In these reports, the materials could exhibit different magnetic behaviors even with a similar chemical stoichiometry. It seems that there are different explanations of the experimental results. Particularly, there is no consensus on the origin of the magnetism. Concerning the magnetic mechanism, one tends to think that the origin of magnetism in these samples is related to the oxygen vacancies and the formation of fluorite crystal structures,[9,11] which could be examined by multi-doped technologies.[12] In order to study the role of oxygen vacancies, Zn and Co multi-doped CeO_2 DMO particles were prepared using the hydrothermal method in Ref. [13] and many oxygen vacancies can be produced in the host lattice, so that the correlations of the oxygen vacancies and magnetic behaviors can be tested. However, the results clearly show that the oxygen vacancies alone are unable to induce ferromagnetic behaviors. Therefore, in this paper, our concerns are the magnetic behaviors of such materials with a similar concentration and a few or no oxygen vacancies. It is known that electrochemical synthesis is an attractive method for making ceramic oxide films and powders because it offers the advantages of low temperature processing, low cost, high purity and controlled microstructure.[14] Particularly, ceria materials pre-

*Project supported by the Natural Science Foundation of Zhejiang Province, China (Grant No. LY12A01002), the National Natural Science Foundation of China (Grant Nos. 11204058 and 21073162), and the Hangzhou Dianzi University, China (Grant No. KYF09150603).

†Corresponding author. E-mail: yingzip@hdu.edu.cn

© 2014 Chinese Physical Society and IOP Publishing Ltd

pared by the anodic electrochemical method are considered to have less oxygen vacancies and less defects in the lattice compared with other fabrication methods.[15] Up to now, few works are found to investigate such ceria-based materials by the anodic electrochemical method. Motivated by this idea, we apply the anodic electrochemical method to study the magnetic mechanism by investigating oxygen vacancies. To this end, we first prepare Zn and Co multi-doped ceria-based materials, then test the mole ratio of oxygen and differentiate between oxygen state in the lattice and at the surface, finally analyze the magnetic behaviors.

2. Experiments

Cerium oxides thin films doped with zinc and cobalt were prepared by using the anodic electrochemical method using a galvanostatic mode at 90 °C, 20 μA/cm^2 for 1 h. The working electrodes were single-sided polished n-type Si (001) wafers. The Si surface was cleaned by chemical HF-ething prior to the electrochemical experiment. Epoxy resin was used on the rear of the Si wafer. Cerium (III) nitrate hexahydrate, zinc nitrate hexahydrate, cobalt nitrate, and ammonium acetate were used as starting materials to prepare the electrolyte. The ratio of the sum of cation ions to ammonium acetate is 1:4, where the zinc concentration is 0.10, and the cobalt concentration is 0.10, 0.20, and 0.30 corresponding to specimens A, B, and C, respectively, as shown in the left column in Table 1. An access amount of saturated sodium hydraoxide solution (NaOH, Yongda Chemical AR) is introduced in the solution to adjust the pH value to about 8 before the electrochemical processing.

Table 1. Mole ratios of the ions by EDS results for the cerium oxide-based thin films with different Co concentrations and their assigned nominal concentrations.

Specimen	Mole ratio of Zn	Mole ratio of Co	Mole ratio of O ($Ce(Zn,Co)O_\delta$)	Assigned nominal $Ce_{1-x}Zn_{0.1}Co_xO_2$
A	0.08	0.04	$\delta = 7$	$x = 0.04$
B	0.08	0.11	$\delta = 6$	$x = 0.11$
C	0.09	0.23	$\delta = 18$	$x = 0.23$

The crystal structures of the specimens were identified by X-ray diffraction (XRD, DX-2500/2600) using Cu $K\alpha$ radiation ($\lambda = 0.15406$ nm). Microstructures of the thin films were characterized by high-resolution transition electron microscopy (HRTEM, Tecnai G2 F30). The specimens were tested by energy dispersive X-ray spectroscopy (EDS) to confirm the expected stoichiometry. Furthermore, X-ray photoelectron spectroscopy (XPS, ESCALAB 250) was used to assess the chemical state of the thin films. All XPS spectra were corrected using the C 1s line at 284.6 eV. A vibrating sample magnetometer of a PPMS (physical property measurement system) with the model 6000 from the Quantum Design Corporation was applied to characterize the magnetic behaviors.

3. Results and discussion

Figure 1 shows the X-ray diffraction patterns of the thin films prepared by the anodic electrochemical method. The scanning range is set from 20° to 65° in order to escape the strong diffraction peak from the Si (001) substrate. For each pattern in Fig. 1, there are five peaks presented in the curve. These diffraction peaks in the pattern can be assigned to a face-centered cubic-phase cerium oxide (JCPDS 34-0394), which correspond to (111), (200), (220), (311), and (222) of cerium oxide with the lattice constant parameters around 0.5440 nm. The value is similar to the reported value for CeO_2. From the XRD results, the peaks from other phases were not observed, which reflected that a cerium oxide-based solid solution was successfully prepared. Though the XRD patterns for specimen A and B were similar, the intensity of the peak (111) for specimen C with a higher Co concentration decreased compared with specimen A and B, revealing more severe distortion of the host lattice in this case. Under our experimental conditions, specimen B is the one with the appropriate Co concentration.

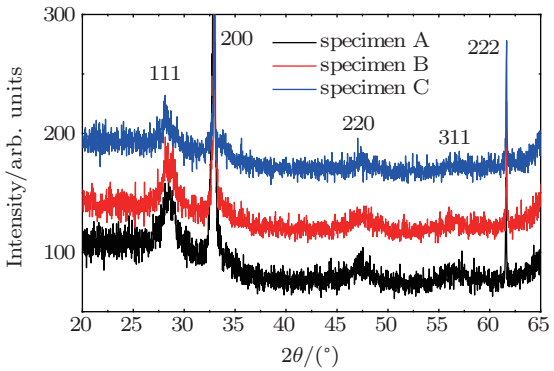


Fig. 1. (color online) X-ray diffraction patterns of the thin films with different Co concentrations prepared by the anodic electrochemical method.

Figures 2(a) and 2(b) show HRTEM images of the specimen B. The clear lattice reveals that a high quality lattice structure with few defects can be observed. The HRTEM cross-section image of the thin film at the interface is shown in Fig. 2(b). The interface between the film and the substrate was found to be smooth and clear. The corresponding diffraction

pattern is shown in Fig. 2(c). It shows clear diffraction dots, which can be assigned to a face-centered cubic-phase cerium oxide. These results suggested that no obvious precipitates were detected for this specimen. Figure 2(d) shows the EDS pattern of specimen B. It can be seen that the elements of O, Ce, and Zn and Co were observed. The experimental results suggest that cerium oxides-based thin films are successfully prepared. Furthermore, the mole ratio of ions can be calculated for different specimens in terms of the EDS results, as shown in Table 1. The calculated Zn ratio roughly agrees with that in the staring solutions, while the calculated Co ratio is different from the value in the starting materials. Note that the mole ratio of oxygen to the total cation ions δ are much larger than 2 (the stoichiometric ratio). Based on the experimental results, there are few oxygen vacancies in the lattice. We need to know that EDS is semi-quantitative and not a precise determination method of the element concentrations. However, the semi-quantitative results can be used to compare the quality of the materials prepared by using different methods.

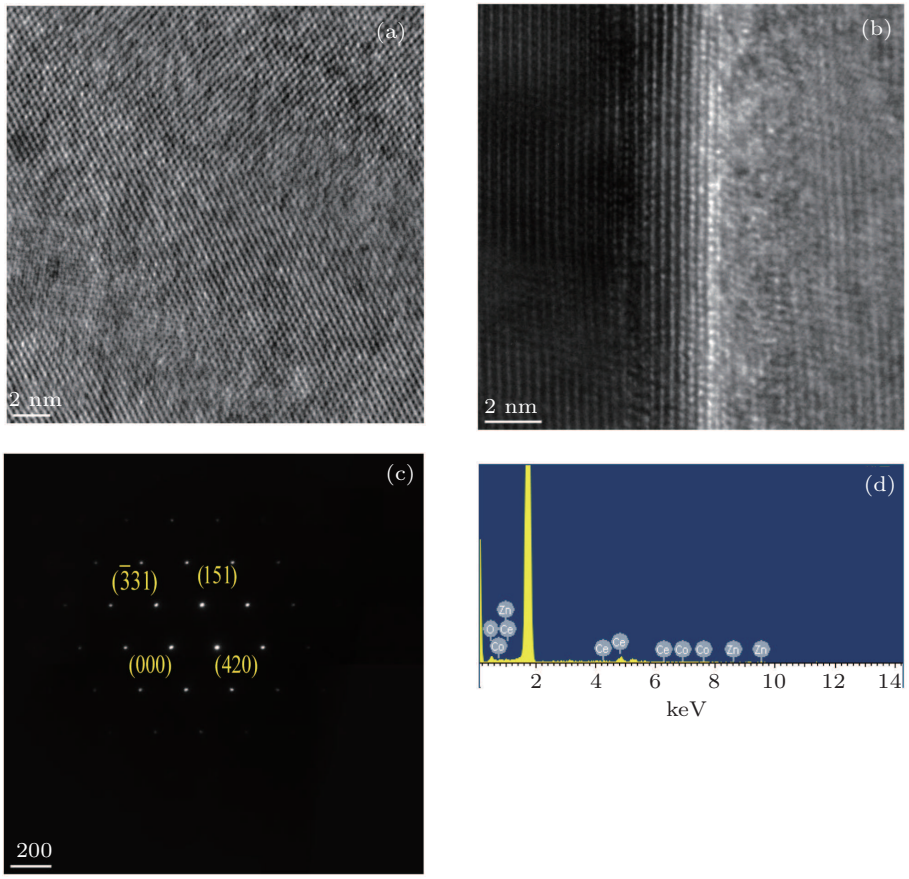


Fig. 2. (color online) HRTEM images of specimen B: (a) the film; (b) the film and substrate at the interface; (c) the corresponding diffraction pattern of the film; (d) EDS pattern of specimen B.

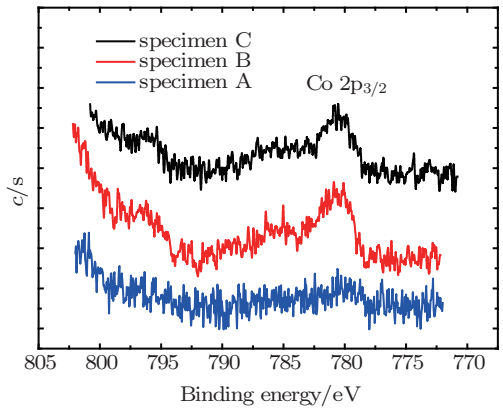


Fig. 3. (color online) XPS Co 2p spectra for the different specimens.

In order to investigate the valence state of the elements and the concentrations for the thin films in detail, we performed XPS characterizations. Figure 3 shows the Co 2p spectra for the cerium oxides doped with Zn and Co with different Co concentrations. It can be seen that for all the spectra, the Co $2p_{3/2}$ peaks appeared at 780 eV, indicating the presence of Co–O bonding in the films.[16] Even for specimen C, the peak locating at 778 eV was not clear, indicating the absence of Co–Co bond.[16]

More detailed investigations were carried out for the specimen B. Figure 4(a) reveals the XPS spectrum Co 2p. The Co $2p_{3/2}$ peak can be observed clearly, while the peak around 795.9 eV which can be assigned to Co $2p_{1/2}$ core level peak

was shaded from an Auger peak Ce MNN nearby. By fitting the Co $2p_{3/2}$ peak with Gaussians (some components of Lorentzian), the spectrum can be resolved into four peaks. The peaks located at 780.1 eV and 781.6 eV correspond to the binding energy of the Co–O bond (nominated to A), as shown in the Fig. 4(a). The presence of two peaks around 780 eV indicates that there are some differences of binding energies for the Co–O bond. It can be explained by the influence of the different Ce–O bonds, i.e., the Ce^{3+} and Ce^{4+} sites. Hence it verifies that Co^{2+} incorporates into the face centered cubic phase cerium oxide lattice at different chemical states. The difference between the peaks for Co $2p_{3/2}$ and Co $2p_{1/2}$ is close to 15.8 eV–14.3 eV, which correspond to the value of cobalt in oxides (around 15.2 eV).[16] The peaks around 785.6 eV and 789.5 eV (nominated to S1 and S2, respectively) correspond to the satellite structures. Under our experimental conditions, the satellite peaks are related to the d-band metal Co, which arise from the interaction between the core hole and the valence electrons O 2p.[17] The satellite peaks reflect the excitation of a valance-band electron from an occupied state to an unoccupied state. Furthermore, the satellite peaks reveal the fact that the substituted Co ions are in the 2+ oxidation states, and there exist the interactions between cobalt and oxygen.

Figure 4(b) presents the O 1s spectrum and its fitting curves with Gaussians (some components of Lorentzian). The lower energy peak $O_{lattice}$ is attributed to the oxide ions in the lattice. While, the peak of the higher energy $O_{surface}$, which locates at 531.3 eV and is believed to be related to the Ce^{3+} ions,[18,19] is due to the effect of O–H.[16] Apparently, the latter is related to the absorptive oxygen bond at the surface, and the absorptive oxygen bond is about 50% of the total oxygen bond by comparing the corresponding peak areas. Even though this is just a semi-quantitative result, it can be applied to explain the reason of the mole ratio of oxygen larger than 2, as illustrated in Table 1. At least from the semi-quantitative analysis, we can know that there are many absorptive oxygen bonds at the surface.

The Ce 3d spectrum can be resolved into many components, as shown in Fig. 4(c), two of which correspond to Ce^{3+} and others correspond to Ce^{4+}. The Ce $3d_{5/2}$ and Ce $3d_{3/2}$ peaks are located with the energy difference of 18.4 eV, which is larger than the corresponding value of Ce in CeO_2.[16] It is due to the effect of Zn and Co in the CeO_2 host lattice. As there is much oxygen in the absorptive state, the actual stoichiomety $\delta' = [O_{lattice}]/[cations]$ (not the nominal stoichiomety $\delta = [O]/[cations]$) can be calculated from the XPS integrated areas of the related elements.[20,21] After extracting the effect of O–H bonds from the O 1s spectrum, the actual stoichiometry $\delta' = [O_{lattice}]/[cation(Ce, Co, Zn)]$ is determined from the XPS integrated areas of the O 1s, Ce 3d, Co 2p, and Zn 2p peaks. The corresponding formula can be written as

$$\delta' = \frac{\text{anion}(O_{lattice})}{\text{cation}(Ce_{3d} + Co_{2p} + Zn_{2p})} = \frac{A_{O_{lattice}}/S_O}{A_{Ce}/S_{Ce} + A_{Co}/S_{Co} + A_{Zn}/S_{Zn}},$$

where $A_{O_{lattice}}$, A_{Ce}, A_{Co}, A_{Zn} are the XPS integrated areas of the $O_{lattice}$ peaks of O 1s, Ce 3d, Co 2p, Zn 2p, and S_O, S_{Ce}, S_{Co}, S_{Zn} are sensitivity factors of O, Ce, Co, and Zn atoms with the values of 8.808, 0.780, 3.59, and 5.589, respectively. The actual stoichiometry δ' is determined to be about 2, which is close to the

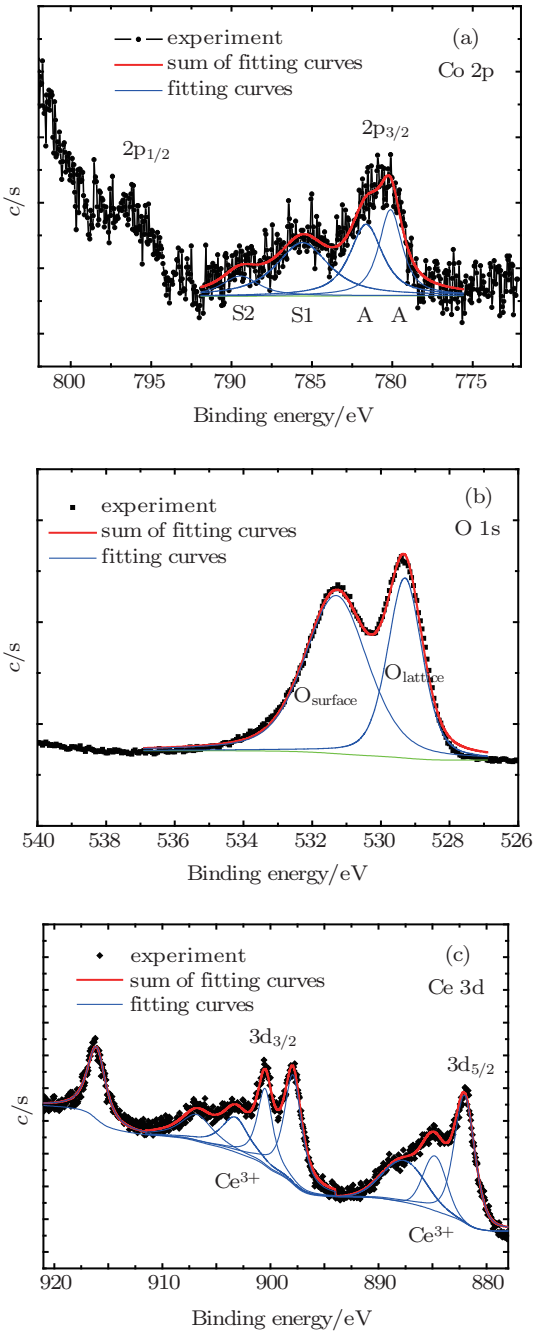


Fig. 4. (color online) XPS spectra of the specimen B with Gaussian fittings in thinner lines: (a) Co 2p XPS spectrum; (b) O 1s XPS spectrum; (c) Ce 3d XPS spectrum.

value of the stoichiometric ratio. In terms of our experimental results, it is reasonable to assign the nominal concentrations $Ce_{1-x}Zn_{0.1}Co_xO_2$ to the thin films with different Co concentrations $x = 0.04$, 0.14, and 0.23, respectively, as shown in Table 1.

Figures 5(a)–5(c) show the *M*–*H* curves measured at 300 K for the $Ce_{1-x}Zn_{0.1}Co_xO_2$ thin films with different Co concentrations. As shown in Fig. 5(a), the saturation magnetization for specimen A is around 4×10^{-5} emu/cm^2. For all the curves, hysteresis loops were observed even in the presence of some noise due to weak signals. It reveals that the *M*–*H* loops are open around the low magnetic field region, as shown in the insets of Fig. 5. It displayed the FM-like behaviors, albeit in somewhat weak magnetization.

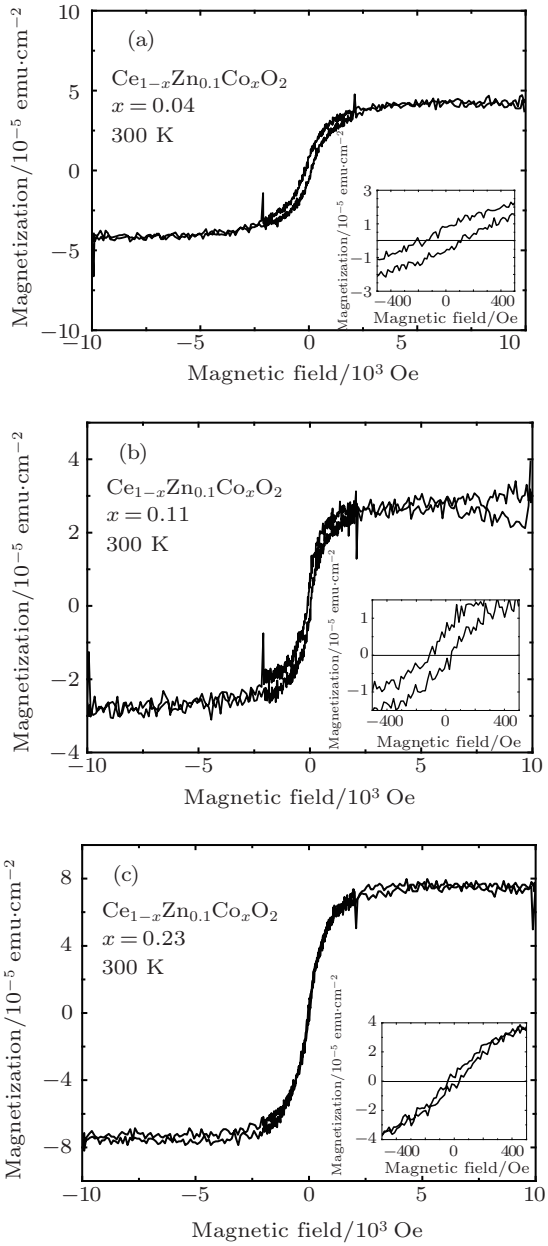


Fig. 5. Magnetization hysteresis loops measured at 300 K for the thin films $Ce_{1-x}Zn_{0.1}Co_xO_2$ with different Co concentrations: (a) Co 0.04; (b) 0.11; (c) 0.23. Inset: enlarged view of the low field region to show the presence of hysteresis and remanence.

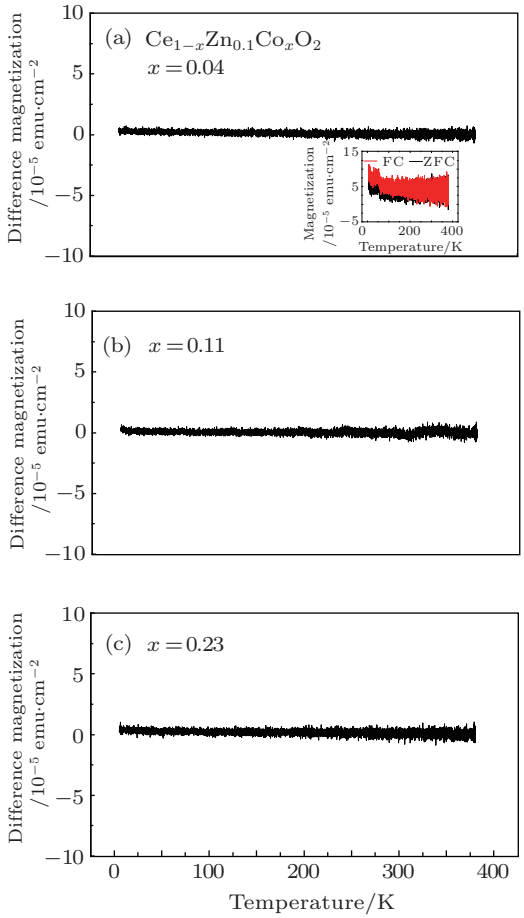


Fig. 6. (color online) Temperature dependence of the different magnetizations between FC and ZFC measured at 100 Oe for the $Ce_{1-x}Zn_{0.1}Co_xO_2$ thin films with Co concentrations $x = 0.04$ (a), 0.11 (b), and 0.23 (c), respectively; inset of panel (a) shows the ZFC (dark) and FC (red) curves for the thin film $Ce_{1-x}Zn_{0.1}Co_xO_2$ ($x = 0.04$) measured at 100 Oe.

To investigate the magnetic behaviors of thin films, we measured the temperature-dependent curves of the magnetization. The specimens were placed in an applied field parallel to the specimen plane at a temperature ranging from 5 K to 380 K. A zero-field-cooled (ZFC) and a field-cooled (FC) method were applied. In our studies, for the FC measurement, measurements of the magnetic moment at each intermediate temperature were carried out at constant applied fields of 100 Oe and 1000 Oe, respectively. The inset of Fig. 6(a) shows the ZFC (dark) and FC (red) curves for the thin film $Ce_{1-x}Zn_{0.1}Co_xO_2$ ($x = 0.04$) measured at 100 Oe. Here it is noted that pink can be observed around 50 K. It is well-known that surface absorptive oxygen, which is present on many samples, gives a magnetic anomaly near 50 K associated with antiferromagnetic ordering. In our case, such a large peak near 50 K claims that there is an absorptive oxygen layer. Though there is some noise, it is still obvious that ZFC and FC curves exhibit almost identical features of the temperature-dependent magnetization. From the FC curve, we can see that the magnetization decreases with temperature, especially at low temperature. The curve obtained in a magnetic field of 100 Oe

shows approximately a zero magnetization up to room temperature, which is in accordance with the *M*–*H* curve with a very weak ferromagnetism. ZFC shows a similar magnetic behavior to that of FC. Furthermore, in terms of the ZFC and FC curves, we can obtain the difference *D* between FC and ZFC. Figures 6(a)–6(c) reveal the temperature-dependence of the *D* values for thin films $Ce_{1-x}Zn_{0.1}Co_xO_2$ with different Co concentrations. Apparently, the values of difference *D* keep a low level. That means that there exists a small ferromagnetic contribution in thin films. Moreover, we will further analyze the temperature-dependent behaviors of the magnetization measured at 1000 Oe. In order to avoid the possible effect of Co precipitates, we choose the results of the specimen with the low Co concentration.

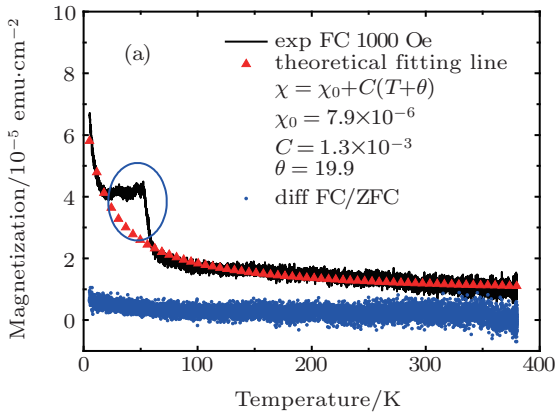


Fig. 7. (color online) Temperature variation of the magnetic magnetization in the FC case measured at 1000 Oe for the thin film $Ce_{1-x}Zn_{0.1}Co_xO_2$ ($x = 0.04$). The scattered point line is the theoretical fitting curve using the modified Curie–Weiss law in terms of the equation $\chi = \chi_0 + C/(T+\theta)$ after getting rid of the peak circled. The lower line shows the different magnetization between FC and ZFC measured at 1000 Oe.

Figure 7 shows the temperature variation of the magnetization in FC and ZFC cases measured at 1000 Oe for the thin film $Ce_{1-x}Zn_{0.1}Co_xO_2$ ($x = 0.04$). It is obvious that the magnetization decreases with the temperature, similar to the feature of metallic behavior. The curve obtained in a magnetic field of 1000 Oe shows a near zero magnetization up to room temperature. ZFC shows a similar magnetic behavior to that of FC, exhibiting a typical outwardly concave shape. Such temperature dependence of magnetization exhibits a Curie-type paramagnetic behavior in these samples, which can be fitted using the modified Curie–Weiss law.[23,24] The experimental data of FC curves at 1000 Oe is fitted to $\chi = \chi_0 + C/(T+\theta)$, where χ_0 is the non-paramagnetic contribution, *C* is the Curie constant, and θ is the Curie–Weiss temperature. As shown in Fig. 7, $\chi_0 = 7.9 \times 10^{-6}$, which is roughly the same order of saturation magnetization for the thin films, indicating that ferromagnetic contributions exist. The positive θ means the existence of an AF interaction, though strong AF behaviors were not observed under the current experimental conditions. The lower line shows the difference *D* of the magnetizations between FC and ZFC cases. It can be seen that the value *D* keeps slowly increasing with decreasing temperature, especially at the low temperature range. It approaches zero when the temperature is close to room temperature. This is accordance with the *M*–*H* loops with the weak ferromagnetic feature.

It is worth comparing the above experimental results with the results obtained in Ref. [13]. In Ref. [13], cerium oxide-based nanoparticles with similar concentrations were prepared using the hydrothermal method, the mole ratio of oxygen to the total cation ions δ is much less than 2, and the percentage of the absorptive oxygen bond is low. Many oxygen vacancies are involved in the host lattice and the *M*–*H* magnetic loops exhibit the paramagnetic behaviors for the cerium oxide-based nanoparticles. Differently, in this paper, the ceria-based thin films were prepared by the anodic electrochemical method. Especially, there are many absorptive oxygen bonds on the surface and few oxygen vacancies in the lattice. It is interesting that weak ferromagnetic behaviors were evidenced by observed *M*–*H* hysteresis loops at room temperature. In terms of these analyses, therefore, the ferromagnetism behaviors of the *M*–*H* loops originate from the absorptive oxygen on the surface rather than the oxygen vacancies in the lattice. The oxygen vacancies alone cannot induce the ferromagnetic properties.[13] We suppose that the magnetic behaviors are related to the absorptive oxygen bond at the surface under our experimental conditions.

4. Conclusion

Zn and Co multi-doped CeO_2-based DMO thin films have been prepared using the anodic electrochemical method. The XRD, HRTEM, and XPS results demonstrate that Zn and Co have been incorporated into the cerium oxides lattice with the face-centered cubic phase inducing two different chemical states of Ce, i.e., Ce^{3+} and Ce^{4+} sites. At the same time, there are many absorptive oxygen bonds at the surface and few oxygen vacancies in the lattice. The absorptive oxygen bond is about 50% of the total oxygen bond by a semi-quantitative method. The value of the actual stoichiomety $\delta' = [O_{lattice}]/[cation(Ce,Co,Zn)]$ is close to 2, which is different from the nominal stoichiomety $\delta = [O]/[cations]$. The *M*–*H* hysteresis loops were observed, exhibiting week ferromagnetism contributions. Furthermore, evidence of relative ferromagnetic contributions was revealed by the temperature dependence of magnetization. It is believed that the ferromagnetic contributions as exhibited in the *M*–*H* loops originate from the absorptive oxygen at the surface rather than the oxygen vacancies in the lattice. In this case, we suppose that the magnetic behaviors are related to the absorptive oxygen at the surface under our experimental conditions.

Acknowledgments

The authors would like to thank Dr. Zhou R B and Zheng L for their help in performing the observations.

References

[1] Tian Y F, Hu S J, Yan S S and Mei L M 2013 *Chin. Phys. B* **22** 088505
[2] Song Y Q, Mu C H, Huo W R, Liu A F, Zhang B and Xiang Y 2013 *Physica B* **413** 92
[3] Phokha S, Pinitsoontorn S and Maensiri S 2012 *J. Appl. Phys.* **112** 113904
[4] Tiwari A, Bhosle V M, Ramachandran S, Sudhakar N, Narayan J, Budak S and Gupta A 2006 *Appl. Phys. Lett.* **88** 142511
[5] Sharma S K, Thakur P, Shalendra K, Shukla D K, Brookes N B, Lee C G, Pirota K R, Koo B H and Knobel M 2010 *Thin Solid Films* **519** 410
[6] Lu Z S, Ma D W, Zhang J, Xu G L and Yang Z X 2012 *Chin. Phys. B* **21** 047505
[7] Colis S, Bouaine A, Schmerber G, Ulhaq-Bouillet C, Dinia A, Choua S and Turek P 2012 *Phys. Chem. Chem. Phys.* **14** 7256
[8] Song Y Q, Zhang H W, Wen Q Y, Li Y X and John Q X 2007 *Chin. Phys. Lett.* **24** 218
[9] Dimri M C, Khanduri H, Kooskora H, Subbi J, Heinmaa I, Mere A, Krustok J and Stern R 2011 *Phys. Status Solidi A* **209** 353
[10] Paunovic N, Popovic Z V and Dohcevic-Mitrovic Z D 2012 *J. Phys.: Condens. Matter* **24** 456001
[11] Thurber A, Reddy K M, Shutthanandan V, Engelhard M H, Wang C, Hays J and Punnoose A 2007 *Phys. Rev. B* **76** 165206
[12] Ma S J, Lu P F, Yu Z Y, Zhao L, Li Q Y, Wu C J and Ding L 2013 *Chin. Phys. B* **22** 037102
[13] Peng Y Z, Bai R, Huo D X and Qian Z H In process
[14] Zhou Y, Philips R J and Switzer J A 1995 *J. Am. Ceram. Soc.* **78** 981
[15] Santamaria M, Asaro L, Bocchetta P, Megna B and Quarto F D 2013 *ECS Electrochem. Lett.* **2** D29
[16] Moulder J F, Stickle W F, Sobol P E and Bomben K D 1995 *Handbook of X-ray Photoelectron Spectroscopy*, *Physical Electronics* (USA) Chap. 8, 30, and 58
[17] Watts J F 1990 *An Introduction to Surface Analysis by Electron Spectroscopy* (Oxford: Oxford University Press) p. 16
[18] Meng F, Wang L and Cui J 2013 *J. Alloy. Compd.* **556** 102
[19] Praline G, Koel B E, Hance R L, Lee H and White J M 1980 *J. Electron Spectrosc.* **21** 17
[20] Meng F, Wang L N and Cui J B 2013 *J. Alloy. Compd.* **556** 102
[21] Zhang F, Wang P, Koberstein J, Khalid S and Chan S W 2004 *Surf. Sci.* **563** 74
[22] Peng Y Z, Liew T, Ye Z Z and Zhang Y Y 2007 *Chin. Sci. Bull.* **52** 2742
[23] Manivannan A, Seehra M S, Majumder S B and Katiyar R S 2003 *Appl. Phys. Lett.* **83** 111
[24] Almeida J M A, Santos P E C, Cardoso L P and Meneses C T 2013 *J. Magn. Magn. Mat.* **327** 185